Journal of Dental Sciences 19 (2024) 1705–1713

Available online at www.sciencedirect.com

ScienceDirect

journal homepage: www.e-jds.com

Dynamic changes in chromatin accessibility during the differentiation of dental pulp stem cells reveal that induction of odontogenic gene expression is linked with specific enhancer construction

Kento Sasaki, Shigeki Suzuki*, Rahmad Rifqi Fahreza, Eiji Nemoto, Satoru Yamada

Department of Periodontology and Endodontology, Tohoku University Graduate School of Dentistry, Sendai, Japan

Received 29 September 2023; Final revision received 20 October 2023; accepted 20 October 2023

Introduction

Chromatin accessibility alteration is a key epigenomic regulatory mechanism of transcription.[1] Histone modifications, such as acetylation, methylation, and phosphorylation, regulate chromatin accessibility by inducing three-dimensional positional changes of histone and the association of histone with DNA. Notably, acetylation of histone H3 in the nucleosomes is highly linked with active gene transcription, and the degree of acetylation is positively and negatively controlled by histone acetyltransferase and histone deacetylase (HDAC).[2]

Dental pulp stem cells (DPSCs) are isolated from permanent teeth by general mesenchymal stem cell markers and possess proliferative properties.[3,4] Furthermore, DPSCs have multi-regenerative abilities,[5–9] and several experimental animal models have shown the usefulness of DPSCs in dental pulp regeneration therapies.[10]

The involvement of epigenetic transcriptional mechanisms in dentin formation has been revealed.[11] Suppression of IκBζ, a newly identified epigenetic modulator, in odontoblasts, promoted dentin formation by inducing dentin extracellular matrix (ECM) organization-related gene expression through the modification of H3K4me3, an open chromatin mark. Recently, we disclosed that the insulator binding sequences were enriched in the accessible chromatin regions adjacent to gene loci of the odonto/osteogenic genes, such as BMP2 and BMPR1B, in differentiating DPSCs.[12] However, integrative interpretation of epigenomic alteration and transcriptome changes during odontogenic differentiation of DPSCs has not been reported.

In this study, by integrating ATAC-seq and RNA-seq analyses of DPSCs before and after odontogenic differentiation, the mechanisms by which epigenomic alteration affects transcriptome changes during odontogenic differentiation were investigated.

* Corresponding author. Department of Periodontology and Endodontology, Tohoku University Graduate School of Dentistry, 4-1, Seiryo-machi, Aoba-ku, Sendai, 980-8575, Japan.
E-mail address: shigeki.suzuki.b1@tohoku.ac.jp (S. Suzuki).

https://doi.org/10.1016/j.jds.2023.10.022

Materials and methods

Cell culture

Human DPSCs were purchased from Lonza Inc. (Walkersville, MD) and cultured in Dulbecco's Modified Eagle Medium (DMEM; Thermo Fisher Scientific, Carlsbad, CA) supplemented with 100 units/ml of penicillin, 100 μg/ml of streptomycin, and 10 % fetal bovine serum (FBS; Biosera, Kansas City, MO). DPSCs were cultivated at 37 °C under humidified atmospheric conditions (5 % CO_2 and 95 % air). For inducing odontogenic differentiation, DPSCs were cultured in the induction medium (DMEM with 10 % FBS, ascorbic acid (100 μg/ml), β-glycerophosphate (10 mM), and dexamethasone (10 nM)) for 24 days.

Alkaline phosphatase (ALP) activity

ALP activity was measured as previously described.[13] Briefly, it was normalized to cell numbers from a parallel cell culture quantified using the Cell Counting Kit-8 (Dojindo, Kumamoto, Japan).[14]

Quantitative PCR (qPCR) analysis

Total RNA purification, cDNA preparation, and qPCR reactions were conducted as described previously.[15] Human *HPRT* was used as an internal reference control. The PCR primer sequences for target genes are shown in Table 1.

ATAC-seq and data analyses

DPSCs were fixed with formaldehyde before and after the 9-day odontogenic induction, and ATAC-seq was performed using the ATAC-Seq Kit (#53150 Active Motif, Carlsbad, CA) following the manufacturer's protocol. Prepared libraries were sequenced using a NovaSeq instrument and 150-bp paired-end reads.[16]

Raw sequence reads were trimmed using Trimmomatic[17] and then PCR duplicates were excluded using MarkDuplicates. The remaining cleaned reads were aligned to a reference genome (hg38) using Bowtie2 version 2.5.1.[18] Duplicate comparisons in sorted BAM files were conducted using the 'multiBamSummary' command in deeptools.[19] Tag directories were generated using the 'makeTagDirectory' command in HOMER,[20] and ATAC-seq peaks were identified using the 'getDiffrentialPeaksReplicates.pl' command in HOMER, specifying '-style region' to generate a high confidence set of peaks across duplicates. The significantly enriched chromatin peaks at day 0 and day 9 were named day-0 open chromatin accessibility peaks (OCAPs) and day-9 OCAPs.

The peaks having significantly higher day-9 tag densities compared with day-0 tag densities were defined as day-9-specific OCAPs, which were identified using the 'getDiffrentialPeaksReplicates.pl' command in HOMER, with biological duplicates of day-9 tag directories as 'sample,' biological duplicates of day-0 tag directories as 'background,' and biological duplicates of the input as 'input.' Similarly, day-0-specific OCAPs were identified using biological duplicates of day-0 tag directories as 'sample,' that of day-9 tag directories as 'background,' and that of input as 'input.' The peaks having equivalent day-0 and day-9 tag densities were defined as overlapping OCAPs.

Peaks were annotated to the nearest genes using the 'annotatePeaks.pl' command in HOMER. Motif predictions were conducted using the 'findMotifsGenoem.pl' command in HOMER to scan the surrounding 200-bp windows. Enhancer predictions were conducted using the 'findMotifsGenoem.pl' command in HOMER, specifying '-style super -o auto -typical'.[20,21] Day-0-specific OCAPs or day-9-specific OCAPs were stitched together into larger regions using default settings. The regions with slope scores greater than 1 were regarded as super-enhancers and those with slope scores less than 1 were regarded as typical-enhancers. To generate the histograms, tags were quantified using the 'annotatePeaks.pl' command in HOMER, with '-size 2000 —hist 10.'

Poly-A selected and strand-specific RNA-seq and data analyses

Purified total RNA was DNase-treated and used in RNA-seq analyses as described previously.[22] For the processing of the RNA-seq data, adapter trimming was conducted using Trim Galore version 0.6.5 (http://www.bioinformatics.babraham.ac.uk/projects/trim_galore/) with default settings and then aligned to a reference genome (hg38) using HISAT2 version 2.2.1.[23] Transcript expression at the exons was quantified using the 'analyzeRepeast.pl' command in HOMER with '-strand both' and '-count exons',

Table 1 Primer pairs used in this study.

Primer name	Species	Direction	Sequence
DSPP	Human	forward	AGAGGACACCCAGAAGCTCA
reverse	GCTGGGACCCTTGATTTCTA		
DMP-1	Human	forward	CCTGTGCTCTCCCAGTAACC
reverse	GCTGTCACTGGGGTCTTCAT		
HPRT	Human	forward	TGGCGTCGTGATTAGTGATG
		reverse	CGAGCAAGACGTTCAGTCCT

DSPP = Dentin sialophosphoprotein, DMP-1 = Dentin matrix protein-1.
HPRT = Hypoxanthine Phosphoribosyltransferase 1.

considering DPSCs collected at day 9 as the target and DPSCs collected at day 0 as the background. The original raw data of ATAC-seq and RNA-seq analyses have been deposited in the NCBI GEO database with accession number GSE244059.

Statistical analysis

Statistical analysis was performed by one-way analysis of variance, followed by the Tukey test (Fig. 1A) and Dunnett's test (Fig. 1B).

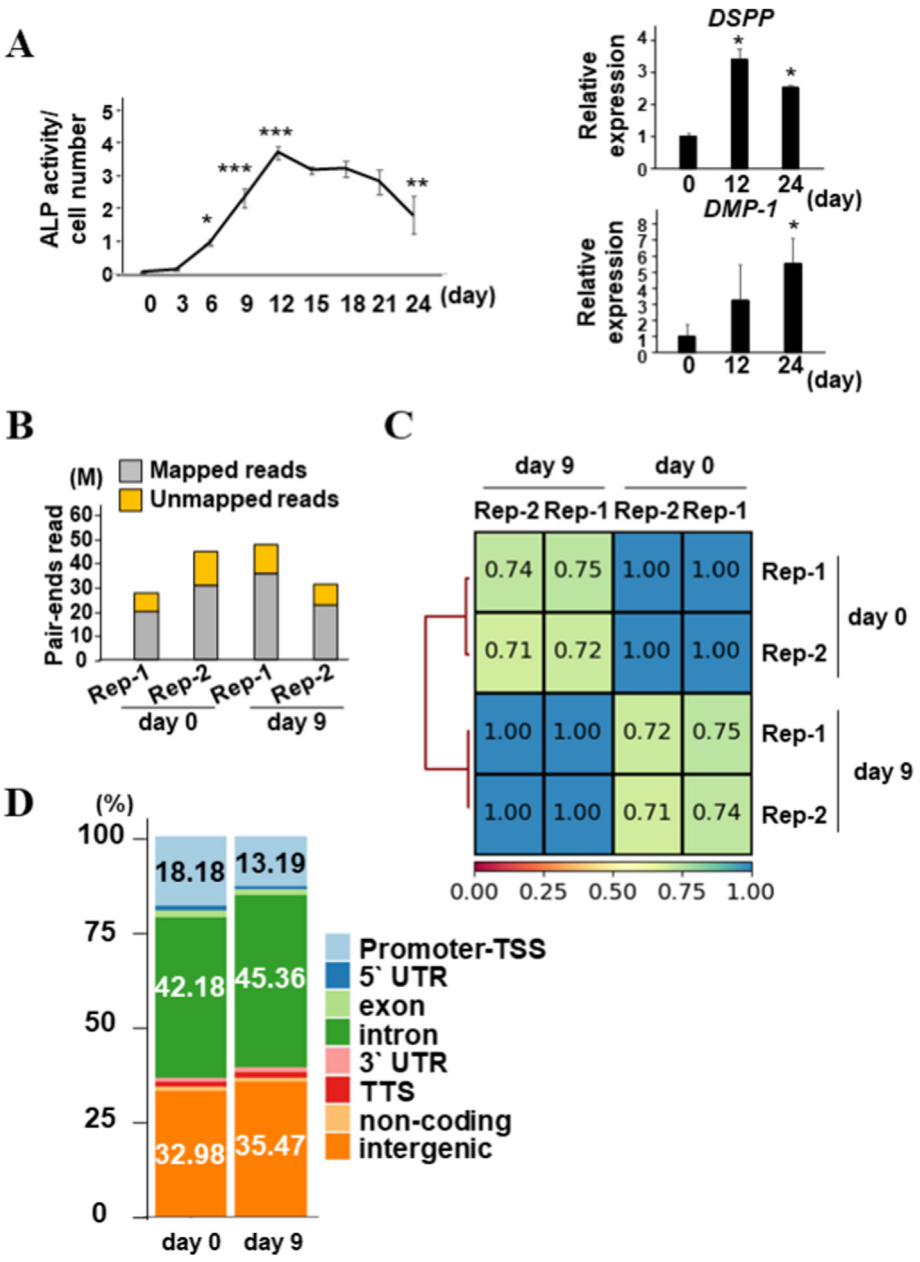

Fig. 1 Enrichment of open chromatin accessible peaks before and after the 9-day odontogenic induction
(A) DPSCs were cultured in an odontogenic induction medium for 24 days, and ALP activity was evaluated. Cell numbers were counted by WST assay, and ALP activities were measured every 3 days. ALP activities were normalized by WST values. Total RNA was collected to quantify the expression of *DSPP* and *DMP-1*. *HPRT* was used for normalization. (B) High-quality read count consisting of the mapping read count (grey) and unmapped read count (yellow) of ATAC-seq are shown. (C) Heatmaps of Spearman's correlation among 2 replicates of day-0 and day-9 samples. (D) Genomic distribution of day-0 OCAPs and day-9 OCAPs. $^{*}P < 0.05$; $^{**}P < 0.01$; $^{***}P < 0.001$ significantly different from the previous day point (A) and higher than day 0 (B). ALP = alkaline phosphatase, Rep = Replicate, 5′UTR = 5′ untranslated region, 3′UTR = 3′ untranslated region, TTS = Transcription termination site. (For interpretation of the references to colour in this figure legend, the reader is referred to the Web version of this article.)

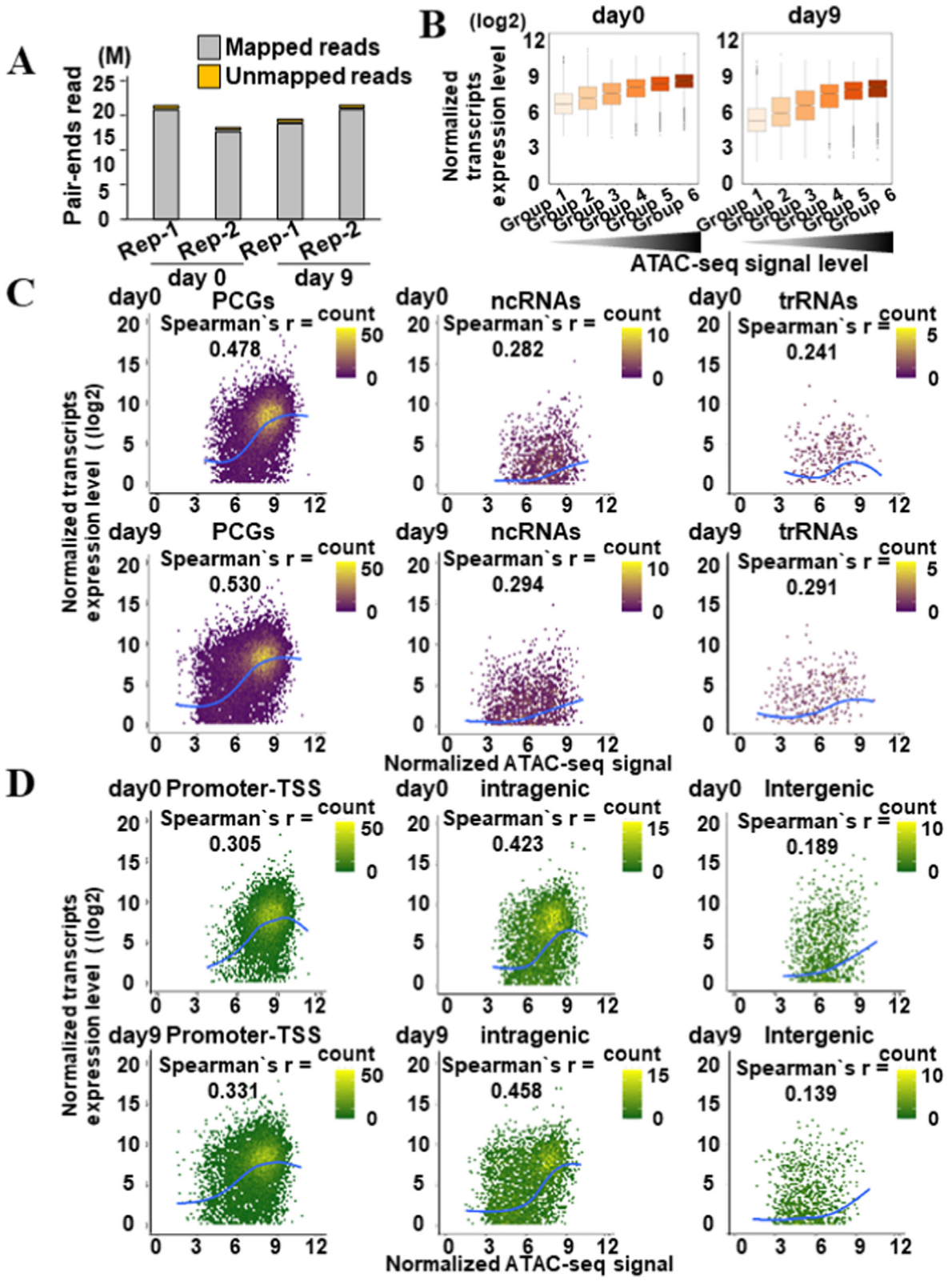

Fig. 2 Integration of transcript expression profile and genomic-wide open chromatin accessible peaks
(A) High-quality read count consisting of the mapping ratio count (grey) and unmapped read count (yellow) of RNA-seq are shown. (B) Increased ATAC-seq signal level is correlated with the average expression level of the nearest transcript at days 0 and 9. (C) Correlation between open chromatin accessible peaks (OCAPs) (measured by normalized ATAC-seq signal) and normalized transcript expression level (obtained by RNA-seq analysis) of PCGs, ncRNAs, and trRNAs. (D) Correlation between OCAPs in the promoter-TSS, intragenic, and intergenic regions (measured by normalized ATAC-seq signal) and normalized transcript expression

Results

Chromatin accessibility changes of DPSCs before and after the 9-day odontogenic differentiation

First, to analyze the odontogenic differentiation abilities, DPSCs were cultured in an odontogenic induction medium for 24 days. The ALP activity, a specific marker of odontogenic differentiation, and the expression changes of *DSPP* and *DMP-1*, fundamental late markers of odontogenic differentiation, were evaluated every 3 days (Fig. 1A). *DSPP* and *DMP-1* were induced on days 12 and 24. ALP activity increased until day 12, with a drastic increase on day 9. Then, whole-genomic open chromatin accessibility alteration before and after the 9-day culture was evaluated. A total of 4 libraries of open chromatin peaks consisting of duplicates of the day 0 and day 9 samples were filtered, deduplicated, and annotated to the human genome (hg38), from which 20.21–36.08 million (M) informative reads survived. The plot correlation analysis indicated complete concurrence of day 0 and day 9 duplicated samples (Fig. 1C). The majority of day-0 OCAPs and day-9 OCAPs were annotated to the intron region (day 0: 42.18 %, day 9: 45.36 %), intergenic region (day 0: 32.98 %, day 9: 35.47 %), and promoter-transcriptional start site (TSS) region (day 0: 18.18 %, day 9: 13.19 %) (Fig. 1D).

Integration of transcriptome and chromatin accessibility analyses

To decipher transcriptional activity regulated by OCAPs during DPSC differentiation, RNA-seq analysis was conducted on days 0 and 9. A total of 4 libraries consisting of duplicates of the day 0 and day 9 samples were filtered and annotated to the human genome (hg38), and 15.83–19.70 M informative reads survived. Higher ATAC-seq signals induced higher expression levels of the nearest transcripts at days 0 and 9 (Fig. 2B). Transcripts were classified into protein-coding genes (PCGs), non-coding RNAs (ncRNAs), which include ncRNA, antisense RNA, and miRNA, and transcripts of regulatory RNAs (trRNAs), which include pseudogenes, rRNA, snoRNA, and snRNA. Then, the correlations between the ATAC-seq signal and the expression levels of PCGs, ncRNAs, and trRNAs were evaluated. The PCG expression level was moderately correlated with chromatin accessibility (day 0: Spearman's $R = 0.478$, day 9: Spearman's $R = 0.530$). Expression levels of ncRNAs and trRNAs were weakly correlated with chromatin accessibility (day 0 ncRNAs: Spearman's $R = 0.282$; day 9 ncRNAs: Spearman's $R = 0.294$; day 0 trRNAs: Spearman's $R = 0.241$; day 9 trRNAs: Spearman's $R = 0.291$) (Fig. 2C).

Next, ATAC-seq peaks were classified by their genomic position. The correlation between the ATAC-seq signal peaks in the promoter-TSS, intergenic, or intragenic regions, which include 5′UTR, exon, intron, 3′UTR, TTS, and non-coding regions in the gene locus, and the transcript expression level were examined regardless of transcript classification. Promoter-TSS peaks were weakly correlated with transcript expression level (day 0: Spearman's $R = 0.305$, day 9: Spearman's $R = 0.331$). Intragenic peaks were moderately correlated with transcript expression level (day 0: Spearman's $R = 0.423$, day 9: Spearman's $R = 0.458$). However, intergenic peaks were barely correlated with RNA expression level (day 0: Spearman's $R = 0.189$, day 9: Spearman's $R = 0.139$). These results indicated the important role of open chromatin in active gene expression, especially for PCGs, and the *cis*-regulatory roles of open chromatin peaks in promoter-TSS and intragenic regions possessed dominant effects in active gene expression.

Day-9-specific OCAPs are strongly associated with transcript expression level

Identified ATAC-seq peaks were classified into day-0-specific OCAPs (7206 peaks), day-9-specific OCAPs (4643 peaks), and overlapping OCAPs (78913 peaks) to explore whether the day-9-specific OCAPs contribute to stage-specific gene expression. The histograms and heatmaps revealed distinct classifications (Fig. 3A). Then, the nearest PCGs, ncRNAs, and trRNAs of day-0-specific OCAPs and day-9-specific OCAPs were separately identified.

The expression ratio (day 9/day 0) of all transcripts was obtained by dividing the normalized expression level at day 9 by that at day 0. As shown in Fig. 3B, the ratio obtained by dividing the average ratio of PCGs associated with day-9-specific OCAPs (5.773 from 1178 peaks) with the average ratio of PCGs associated with day-0-specific OCAPs (1.597 from 2530 peaks) was 3.615 folds. Similarly, the ratio obtained by dividing the average ratio of ncRNAs associated with day-9-specific OCAPs (3.060 from 89 peaks) with the average ratio of ncRNAs associated with day-0-specific OCAPs (2.072 from 147 peaks) was 1.477 folds. The ratio obtained by dividing the average ratio of trRNAs associated with day-9-specific OCAPs (1.166 from 6 peaks) with the average ratio of trRNAs associated with day-0-specific OCAPs (1.325 from 16 peaks) was 0.880 folds. The ratios of PCGs (3.615 folds), ncRNAs (1.477 folds), and trRNAs (0.880 folds) imply that day-9-specific OCAPs contributed to stage-specific PCG and ncRNA expression.

Next, the correlation between the peak positional classification and the transcript expression level was analyzed. As shown in Fig. 3C, the ratio obtained by dividing the average ratio of transcripts associated with day-9-specific OCAPs in the promoter-TSS region (104.583 from 57 peaks) with the average ratio of PCGs associated with day-0-specific OCAPs in the promoter-TSS region (0.879 from 108 peaks) was 118.980. Similarly, the ratio obtained by dividing the average ratio of transcripts associated with day-9-specific-OCAPs in the intragenic region (2.454 from 1116 peaks) with the average ratio of transcripts associated with day-0-specific OCAPs in the intragenic region (1.561 from 1719 peaks) was 1.572. The ratio obtained by dividing

level (obtained by RNA-seq analysis). PCGs = Protein coding genes, ncRNAs = non-coding RNAs, trRNAs = transcripts of regulatory RNAs. Promoter-TSS = Promoter-transcription start site. (For interpretation of the references to colour in this figure legend, the reader is referred to the Web version of this article.)

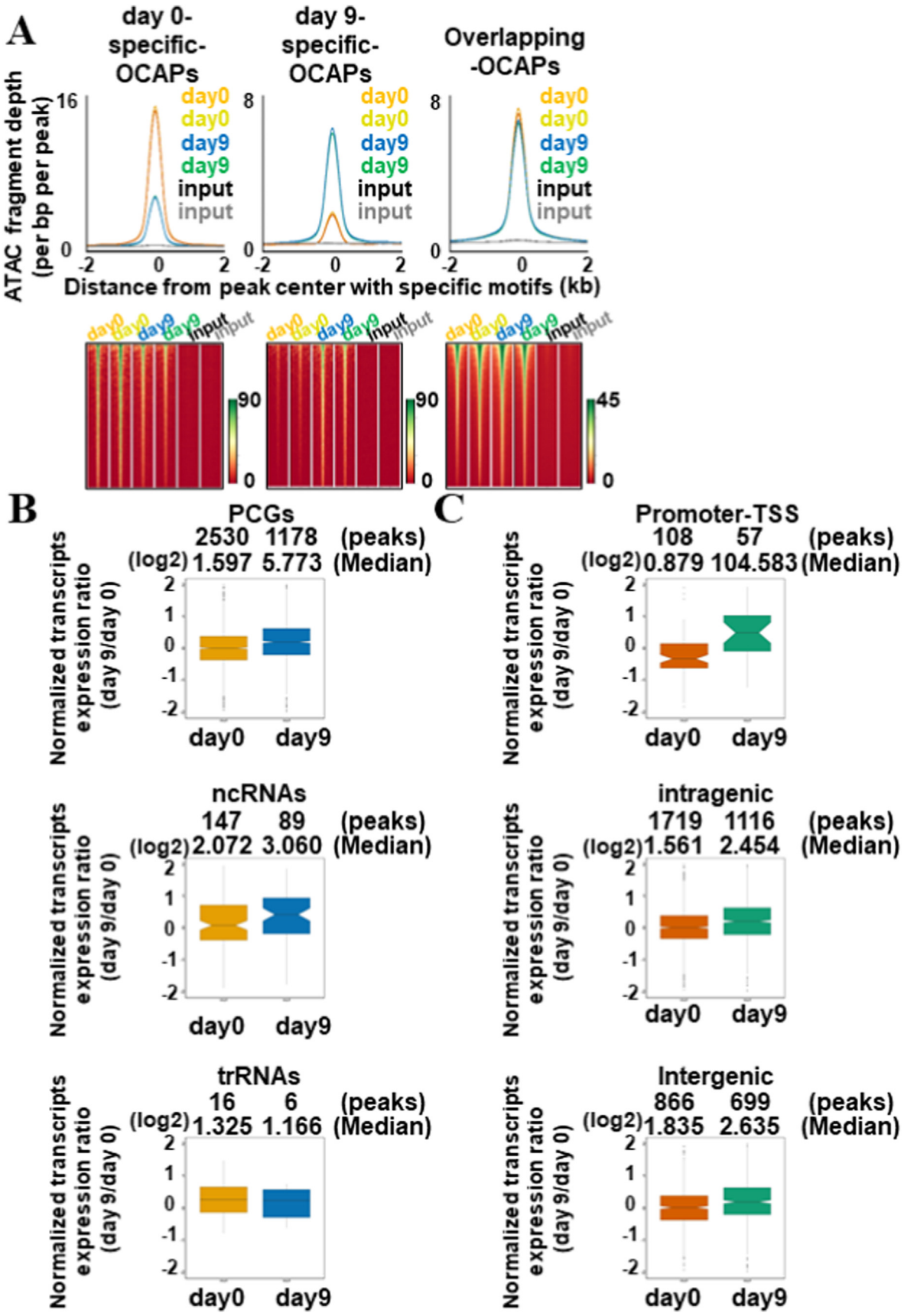

Fig. 3 Day-9-specific OCAPs are strongly associated with transcript expression level

(A) Histograms and heatmaps of ATAC-seq signals of day-0-specific OCAPs, day-9-specific OCAPs, and overlapped OCAPs in 4-kb

the average ratio of transcripts associated with day-9-specific OCAPs in the intergenic region (2.635 from 699 peaks) with the average ratio of transcripts associated with day-0-specific OCAPs in the intergenic region (1.835 from 866 peaks) was 1.436. According to the resultant ratios of OCAPs in promoter-TSS (118.980 folds), OCAPs localized in the intragenic region (1.572 folds), and OCAPs localized in the intergenic region (1.436 folds), chromatin accessibility status at day 9 in the promoter-TSS region was strongly linked with transcript expression level.

The super-enhancer region is constructed in the *ALPL* gene locus at day 9

To investigate whether day-9-specific OCAPs play a critical role in DPSC differentiation, gene ontology (GO) analyses of neighboring genes were conducted (Fig. 4A). Most of the enriched terms, such as Adipogenesis, TGF-beta signaling pathway, Ectoderm differentiation, Focal adhesion, and Mesodermal commitment pathway, were commonly enriched from day-0-specific OCAPs and day-9-specific OCAPs. Several terms, such as Bone morphogenic protein (BMP) signaling, Regulation angiopoietin-like protein 8 regulatory pathway, and Leptin signaling pathway, were selectively enriched in day-9-specific OCAPs.

The number of super- and typical-enhancers was drastically enriched in day-9-specific OCAPs (super:124 regions, typical: 3704 regions) compared with day-0-specific OCAPs (super: 9 regions, typical: 532 regions) (Fig. 4B). One of the 124 super-enhancers was constructed in the *ALPL* gene locus, which is highlighted with a light grey mesh and dashed line in Fig. 4C. In the *ALPL* gene locus on day 9, a total of 11 OCAPs were identified, marked with red reverse triangles in Figs. 4C and 2 of them were day-9-specific OCAPs, as highlighted with a dark grey mesh. Both these peaks contain the Smad4 consensus element, which was only detected in these 2 OCAPs, among the 11 OCAPs.

Discussion

In this study, we profiled chromatin accessibility in conjunction with transcriptomic analysis before and after the odontogenic differentiation and revealed that, at day 9, higher numbers of super- and typical-enhancers were constructed close to key differentiation maker genes such as *ALPL* (Fig. 4). The degree of chromatin accessibility was proportional to the expression level of neighboring transcripts, including PCGs and ncRNAs (Fig. 2). ncRNAs are generally involved in key cellular functions[24–26] and act as transcriptional regulators by guiding transcriptional factor complexes into specific gene loci and modulating subcellular protein localization, thereby regulating cellular properties such as proliferation and migration.

The number of differentially day-0-specific OCAPs and day-9-specific OCAPs account for a small population of the total peaks (Fig. 3). This unexpectedly lower number of differentially enriched peaks indicated that particular chromatin peaks close to key differentiation marker genes were selectively altered, but the majority of the chromatin peaks associated with basic cellular functions were unchanged. The angiopoietin-like protein 8 (ALP8) regulatory pathway was identified as an enriched pathway of day-9-specific OCAPs (Fig. 4). ALP8 is functionally related to pro-inflammation and ECM degradation.[27] Generally, DPSCs possesses anti-inflammatory ability, but as dental pulp fibroblasts secrete pro-inflammatory extracellular vesicle,[28] differentiated DPSCs may possess a similar pro-inflammatory base. ALP8-induced ECM degradation might facilitate ECM turnover during cyto-differentiation of DPSCs. Herein, expression of *DSPP* and *DMP-1* was induced (Fig. 1). Their transcribed products are two highly phosphorylated dentin/pulp ECM proteins[29,30] and have prominent roles in odontogenic differentiation, dentin mineralization, and anti-inflammation.[31–36] One overlapping OCAP was identified in the intergenic region between *DMP-1* and *DSPP* gene loci. Thus, further study is necessary to identify the TF association and 3D distance of this OCAP to the *DMP-1* and *DSPP* promoter regions by 4C-seq analysis. The Leptin signal pathway was also enriched in day-9-specific OCAPs (Fig. 4A). Leptin is known to induce osteoblastic differentiation,[37] and therefore, similar promoting effects of the Leptin signaling pathway in odontogenic differentiation of DPSCs can be expected.

On day 9, super-enhancer regions were constructed in the *ALPL* gene locus, and two Smad binding elements were specifically identified as day-9-specific OCAPs localized in this super-enhancer region. The increased numbers of super- and typical-enhancers after the differentiation are critical factors for the dominant correlation between chromatin accessibility and transcript expression level at day 9 (Fig. 3C). This trend was most distinct when OCAPs were localized in the promoter-TSS region. To verify the enhancer activity of the identified super-enhancer regions, further studies, such as HiC-seq, which discloses three-dimensional genomic architecture, and CRISPR/dCas9-based epigenetic editing systems, which change the

windows centered on the peaks. The lines in histograms represent values of normalized ACAC-seq tag enrichment of duplicate samples for day 0, day 9, and input. (B) Nearest PCGs, ncRNAs, and trRNAs of day-0-specific OCAPs and day-9-specific OCAPs are extracted. Then, their expression level at day 9 is divided by that at day 0 to obtain the day 9/day 0 ratio. A comparison of the day 9/day 0 ratio for day-0-specific OCAP-associated and day-9-specific OCAP-associated PCGs, ncRNAs, and trRNAs is shown. Peak numbers and median values are shown above the plots. (C) Nearest transcripts of day-0-specific OCAPs and day-9-specific OCAPs in the promoter-TSS, intragenic, and intergenic regions are extracted. Then, the expression level of the nearest transcripts at day 9 is divided by that at day 0 to obtain the day 9/day 0 ratio. A comparison of the day 9/day 0 ratio for the transcripts associated with day-0-specific OCAPs and day-9-specific-OCAPs in promoter-TSS, intragenic, and intergenic regions is shown. Peak numbers and median values are shown above the plots. OCAPs = open chromatin accessibility peaks, PCGs = Protein coding genes, ncRNAs = non-coding RNAs, trRNAs = transcripts of regulatory RNAs. Promoter-TSS = Promoter-transcription start site.

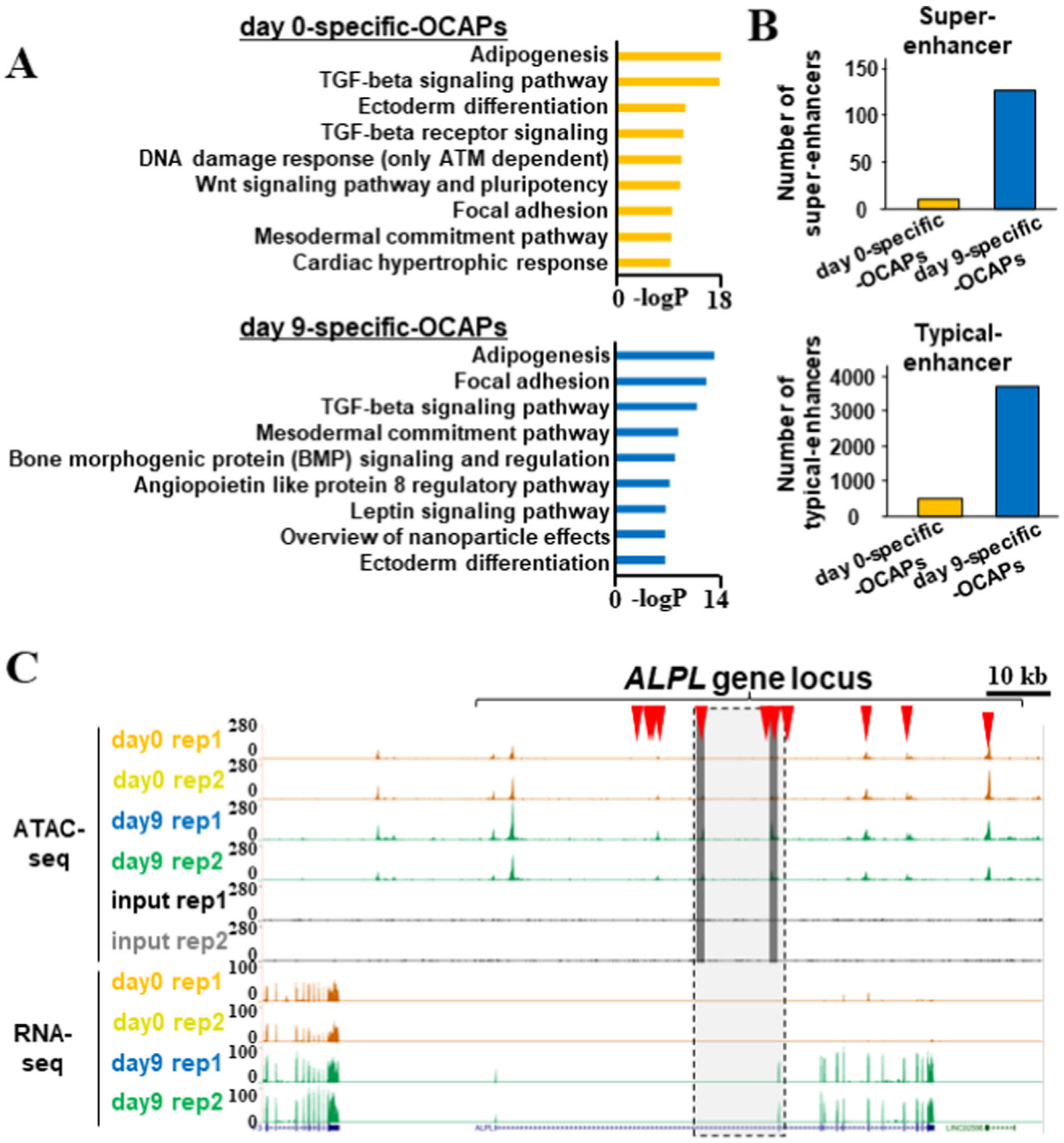

Fig. 4 The super-enhancer region is constructed in the *ALPL* gene locus on day 9
(A) Top 9 pathways of nearest transcripts of day-0 OCAPs and day-9 OCAPs. (B) Numbers of super- and typical-enhancers in day-0-specific OCAPs and day-9-specific OCAPs. (C) UCSC Genomic Browser track of *ALPL* gene locus shows drastic exon-specific tag accumulation in day 9 duplicate samples but not in day 0 duplicates. OCAPs identified on day 9 are indicated by red arrowheads, as shown on the top of the genome track. A light grey mesh area surrounded by a dashed line indicates the super-enhancer region constructed on day 9. Two dark grey areas indicate day-9-specific OCAPs. OCAPs = open chromatin accessibility peaks. (For interpretation of the references to colour in this figure legend, the reader is referred to the Web version of this article.)

accessibility of targeting enhancers by using specific sgRNAs,[38] are necessary.

In conclusion, a specific local chromatin region was selectively opened in differentiating DPSCs, and particularly, super-enhancers were generated, which guided differentiative TFs, such as Smad1/4, to their target sites. Therefore, integrative data on chromatin accessibility and transcriptome of DPSCs can help us understand odontogenic differentiation of DPSCs.

Declaration of competing interest

The authors declare that there are no conflicts of interest.

Acknowledgments

The present study was financially supported by JSPS KAKENHI Grant Number 22H03266 and 22K19611 for Shigeki

Suzuki and 20H03862, 20K21668, and 23K18350 for Satoru Yamada.

References

1. Li B, Carey M, Workman JL. The role of chromatin during transcription. Cell 200723;128:707-719..
2. Kouzarides T, Bannister AJ. Regulation of chromatin by histone modifications. *Cell Res* 2011;21:381—95.
3. Gao Y, Tian Z, Liu Q, et al. Neuronal cell differentiation of human dental pulp stem cells on synthetic polymeric surfaces coated with ECM proteins. *Front Cell Dev Biol* 2022;10:893241.
4. Yoshida K, Suzuki S, Yuan H, et al. Public RNA-seq data-based identification and functional analyses reveal that MXRA5 retains proliferative and migratory abilities of dental pulp stem cells. *Sci Rep* 2023;13:15574.
5. Sun Q, Si-Chen RB, Zhuang, Z, et al. Lysine demethylase 3A promotes chondrogenic differentiation of aged human dental pulp stem cells. J Dent Sci (2023)..
6. Heo SC, Keum BR, Seo EJ, et al. Lysophosphatidic acid induces proliferation and osteogenic differentiation of human dental pulp stem cell through lysophosphatidic acid receptor 3/extracellular signal-regulated kinase signaling axis. *J Dent Sci* 2023;18:1219—26.
7. Kim Y, Park HJ, Kim M-K, et al. Naringenin stimulates osteogenic/odontogenic differentiation and migration of human dental pulp stem cells. *J Dent Sci* 2023;18:577—85.
8. Jin C, Zhao S, Xie H. Forskolin enhanced the osteogenic differentiation of human dental pulp stem cells in vitro and in vivo. *J Dent Sci* 2023;18:120—8.
9. Lim HM, Nam MH, Kim YM, Seo YK. Increasing odontoblast-like differentiation from dental pulp stem cells through increase of β-catenin/p-GSK-3β expression by low-frequency electromagnetic field. *Biomedicines* 2021;9:1049.
10. Kwack KH, Lee HW. Clinical potential of dental pulp stem cells in pulp regeneration: current endodontic progress and future perspectives. *Front Cell Dev Biol* 2022;10:857066.
11. Yuan H, Suzuki S, Terui H, et al. Loss of IκBζ drives dentin formation via altered H3K4me3 status. *J Dent Res* 2022;101:951—61.
12. Suzuki S, Hasegawa R, Sato A, et al. Chromatin accessibility analysis reveals functional transcriptional factors and regulators in dental pulp stem cell differentiation. *Jpn J Conserv Dent* 2023;66:179—91 [In Japan, English abstract].
13. Hirata-Tsuchiya S, Suzuki S, Okamoto K, et al. A small nuclear acidic protein (MTI-II, Zn2+-binding protein, parathymosin) attenuates TNF-α inhibition of BMP-induced osteogenesis by enhancing accessibility of the Smad4-NF-κB p65 complex to Smad binding element. *Mol Cell Biochem* 2020;469:133—42.
14. Yoshida K, Suzuki S, Kawada-Matsuo M, et al. Heparin-LL37 complexes are less cytotoxic for human dental pulp cells and have undiminished antimicrobial and LPS-neutralizing abilities. *Int Endod J* 2019;52:1327—43.
15. Yamamoto T, Yuan H, Suzuki S, Nemoto E, Saito M, Yamada S. Procyanidin B2 enhances anti-inflammatory responses of periodontal ligament cells by inhibiting the dominant negative pro-inflammatory isoforms of Peroxisome proliferator-activated receptor. J Dent Sci (2023)..
16. Bai J, Lin Y, Zhang J, et al. Profiling of chromatin accessibility in pigs across multiple tissues and developmental stages. *Int J Mol Sci* 2023;24:11076.
17. Bolger AM, Lohse M, Usadel B. Trimmomatic: a flexible trimmer for Illumina sequence data. *Bioinformatics* 2014;30:2114—20.
18. Langmead B, Salzberg SL. Fast gapped-read alignment with Bowtie 2. *Nat Methods* 2012;9:357—9.
19. Ramírez F, Dündar F, Diehl S, Grüning BA, Manke T. deepTools: a flexible platform for exploring deep-sequencing data. *Nucleic Acids Res* 2014;42. W187—W91.
20. Heinz S, Benner C, Spann N, et al. Simple combinations of lineage-determining transcription factors prime cis-regulatory elements required for macrophage and B cell identities. *Mol Cell* 2010;38:576—89.
21. Whyte WA, Orlando DA, Hnisz D, et al. Master transcription factors and mediator establish super-enhancers at key cell identity genes. *Cell* 2013;153:307—19.
22. Yuan H, Suzuki S, Hirata-Tsuchiya S, et al. PPARγ-induced global H3K27 acetylation maintains osteo/cementogenic abilities of periodontal ligament fibroblasts. *Int J Mol Sci* 2021;22:8646.
23. Kim D, Langmead B, Salzberg SL. HISAT: a fast spliced aligner with low memory requirements. *Nat Methods* 2015;12:357—60.
24. Suzuki S, Yamada S. Epigenetics in susceptibility, progression, and diagnosis of periodontitis. *Jpn Dent Sci Rev* 2022;58:183—92.
25. Suzuki S, Yuan H, Hirata-Tsuchiya S, et al. DMP-1 promoter-associated antisense strand non-coding RNA, panRNA-DMP-1, physically associates with EGFR to repress EGF-induced squamous cell carcinoma migration. *Mol Cell Biochem* 2021;476:1673—90.
26. Suzuki S, Hoshino H, Yoshida K, et al. Genome-wide identification of chromatin-enriched RNA reveals that unspliced dentin matrix protein-1 mRNA regulates cell proliferation in squamous cell carcinoma. *Biochem Biophys Res Commun* 2018;495:2303—9.
27. Liao Z, Wu X, Song Y, et al. Angiopoietin-like protein 8 expression and association with extracellular matrix metabolism and inflammation during intervertebral disc degeneration. *J Cell Mol Med* 2019;23:5737—50.
28. Suzuki S, Fukuda T, Nagayasu S, et al. Dental pulp cell-derived powerful inducer of TNF-α comprises PKR containing stress granule rich microvesicles. *Sci Rep* 2019;9:3825.
29. Suzuki S, Haruyama N, Nishimura F, Kulkarni AB. Dentin sialophosphoprotein and dentin matrix protein-1: two highly phosphorylated proteins in mineralized tissues. *Arch Oral Biol* 2012;57:1165—75.
30. Suzuki S, Nakanishi J, Yoshida K, Shiba H. Dentin sialophosphoprotein is a potentially latent bioactive protein in dentin. *J Oral Biosci* 2016;58:134—42.
31. Li W, Chen L, Chen Z, et al. Dentin sialoprotein facilitates dental mesenchymal cell differentiation and dentin formation. *Sci Rep* 2017;7:300.
32. Suzuki S, Sreenath T, Haruyama N, et al. Dentin sialoprotein and dentin phosphoprotein have distinct roles in dentin mineralization. *Matrix Biol* 2009;28:221—9.
33. Jaha H, Husein D, Ohyama Y, et al. N-terminal dentin sialoprotein fragment induces type I collagen production and upregulates dentinogenesis marker expression in osteoblasts. *Biochem Biophys Rep* 2016;6:190—6.
34. Suzuki S, Kobuke S, Haruyama N, Hoshino H, Kulkarni AB, Nishimura F. Adhesive and migratory effects of phosphophoryn are modulated by flanking peptides of the integrin binding motif. *PLoS One* 2014;9:e112490.
35. Kobuke S, Suzuki S, Hoshino H, et al. Relationship between length variations in Ser/Asp-rich repeats in phosphophoryn and in vitro precipitation of calcium phosphate. *Arch Oral Biol* 2015;60:1263—72.
36. Nakanishi J, Suzuki S, Yoshida K, et al. Dentin phosphoprotein inhibits lipopolysaccharide-induced macrophage activation independent of its serine/aspartic acid-rich repeats. *Arch Oral Biol* 2020;110:104634.
37. Zeadin MG, Butcher MK, Shaughnessy SG, Werstuck GH. Leptin promotes osteoblast differentiation and mineralization of primary cultures of vascular smooth muscle cells by inhibiting glycogen synthase kinase (GSK)-3β. *Biochem Biophys Res Commun* 2012;425:924—30.
38. Li K, Liu Y, Cao H, et al. Interrogation of enhancer function by enhancer-targeting CRISPR epigenetic editing. *Nat Commun* 2020;11:485.